**Journal of Mathematical Modeling**
Vol. -, No. -, 2021, pp. -

JMM

# The approximate solution of one dimensional stochastic evolution equations by meshless methods

**Mahdi Jalili, Rezvan Salehi***
Department of Applied Mathematics, Faculty of Mathematical SciencesTarbiat Modares University, P.O. Box 14115-134, Tehran, Iran
*Email(s): mahdi_jalili@modares.ac.ir, r.salehi@modares.ac.ir*

**Abstract.** In this article, we develop an iterative scheme based on the meshless methods to simulate the solution of one dimensional stochastic evolution equations using radial basis function (RBF) interpolation under the concept of Gaussian random field simulation. We use regularized Kansa collocation to approximate the mean solution at space and the time component is discretized by the global $\theta$-weighted method. Karhunen-loève expansion is employed for simulating the Gaussian random field. Statistical tools for numerical analysis are standard deviation, absolute error, and root mean square. In this work, we solve two major problems for showing the convergence, and stability of the presented method on two problems. The first problem is the semilinear stochastic evolution problem, and the second one is stochastic advection-diffusion model with different control values.

*Keywords*: Stochastic partial differential equation, Gaussian random field, meshless method, radial basis function, regularized Kansa collocation, reproducing kernel Hilbert space.
*AMS Subject Classification 2010*: 34A34, 65L05.

## 1 Introduction

The randomness of nature can be seen in every particle and most of these particles have a dynamic where mathematician can model these dynamics by partial differential equations. Real-world dynamical systems have a stochastic source which these models are so-called stochastic partial differential equations (SPDEs). A lot of challenges exist through modeling and simulation of SPDEs but the most important and hard challenge is finding an analytical solution to SPDEs. In the last two decades, the usability of numerical methods to approximate the solution of SPDEs has been shown extreme growth.

In the last two decades, many numerical methods have been employed to find the mean solution of SPDEs where some variations of them are finite difference, finite element, chaos

*Corresponding author.
Received: 13 January 2021 / Revised: 16 February 2021 / Accepted: 16 February 2021
DOI: 10.22124/jmm.2021.18624.1594

 

expansions, and spectral methods. Any of these numerical methods need to have a connection between the world of approximation and the space of the stochastic process.

The area of meshless methods structured on reproducing kernel Hilbert space (RKHS) has a strong connection with the stochastic process since all of the stochastic process defined on a probability space like $(\Omega_x, \mathcal{F}_x, \mathbb{F}_x)$ filtered on time by $\mathcal{F}_t$ can be generated by spatial covariance functions selected from RBFs. For more details see [1]. Additionally, the Karhunen-Loève expansion (approach) for simulation of stochastic process needs the Mercer representation theorem which is defined on RKHS.

Various numerical methods are applied to find the approximate solution of one dimensional SPDEs. For instance, finite difference methods (FDM), finite element methods (FEM) [10,11,14], method of lines (MOL) [16] and spectral chaos expansion (SCE) [9]. But these methods have some disadvantages like dimensionality and non-stability. The main objective of using meshless methods is to handle these problems. Previous works on meshless methods for approximate solution of SPDEs can be found in [2–7].

In this paper, we present a straightforward form of the collocation method based on RBF interpolation to approximate the solution of SPDEs. After discretizing the problem in time, we apply the regularized Kansa approach to solve the obtained stochastic boundary-value problem. Indeed, we simulate the stochastic part by Karhune-Loève expansion and develop an iterative scheme to approximate the solution of SPDE. Then by using the exact solution and concepts of Gaussian random field (GRF) and employing statistical tools, we numerically present convergence, stability, and efficiency of our method.

The paper is organized as follows. In Section 2, we discuss the main problem and present stochastic descriptions. In Section 3, we discuss the previous meshless methods in detail. In Section 4, we present the regularized Kansa collocation method for solving boundary-value problems. In Section 5, we develop an iterative scheme for applying discussed method in Section 4 on SPDEs. in Section 6, we solve some numerical examples and report some results. In Section 7, we note some major conclusions of the current work.

## 2 Object problem

In this work, we study the one dimensional stochastic evolution equations formulated as:

$$\frac{\partial U}{\partial t} = \mathcal{A}U + f + \sigma \frac{\partial W}{\partial t}, \qquad \text{on } [a,b] \times [0,T], \tag{1}$$

where $\mathcal{A}$ is linear differential operator, $f$ is deterministic source function, $W$ is time-spatial $Q$-Wiener process, and $\sigma$ is noise level. The $Q$-Wiener process has major properties as defined below.

**Definition 1.** *A $\mathbb{R}^d$-valued stochastic process $\{W(t,\boldsymbol{x}) : t \geq 0\}$ is a $Q$-Wiener process if:*

1. *$W(0,\boldsymbol{x}) = 0$;*
2. *$W(t,\boldsymbol{x})$ is a continuous function $(\mathbb{R}^+)^d \to \mathbb{R}^d$ for each trajectory (sample path) $\omega \in \Omega_x$;*
3. *$W(t,\boldsymbol{x})$ is $\mathcal{F}_t$-adapted and $W(t,\boldsymbol{x}) - W(s,\boldsymbol{x})$ is independent of $\mathcal{F}_s$ for $s < t$;*

*4.* $W(t,\boldsymbol{x}) - W(s,\boldsymbol{x}) \sim Normal(0,(t-s)Q(\boldsymbol{x})), \qquad \forall\ 0 \leq s \leq t.$

Theoretical aspects of the $Q$-Wiener process are very useful but in applied settings, we need to numerically discretize the process. Some of the numerical approaches to simulate the $Q$-Wiener process are the Fourier series, Mercer representation, and Karhunen-Loève expansion. In this work, we choose Karhunen-Loève expansion since it has very fast convergence in Hilbert space. Also, we set all of the theory in RKHS, because of the good results of the eigenvalue structure of Karhunen-Loève expansion.

**Theorem 1.** *[15] Let $W(t,\boldsymbol{x})$ be the $Q$-Wiener process. Then Karhunen-Loève expansion (approach) of $W(t,\boldsymbol{x})$ is:*

$$W(t,\boldsymbol{x}) = \sum_{j=1}^{\infty} \sqrt{q_j}\psi_j(\boldsymbol{x})\beta_j(t), \qquad a.s., \tag{2}$$

*where $\beta_j(t)$ is independent identical distributed(i.i.d) $\mathcal{F}_t$-Brownian motions, $q_j$ and $\psi_j(\boldsymbol{x})$ are corresponding eigenvalues and eigenfunctions, respectively.*

The spatial covariance function $Q$ in the definition of $Q$-Wiener process can be any RBF but to have similarity with literature we set the inverse multiquadric function for coloring Wiener process.

## 3 Previous works

Meshless methods have been widely used in various areas such as interpolation, finding solution of ODEs and PDEs, artificial intelligence, and statistical smoothing. Kansa collocation method which was first introduced by Kansa in [12] is one of the fastest and most flexible methods for solving ODE/PDE problems based on RBF interpolation. The firstly introduced Kansa collocation method is named asymmetric Kansa and applied for a strong form approximation of problems. Fasshauer in [8] developed a symmetric Kansa collocation based on Hermite-RBF interpolation which has some good and bad properties. The most important advantage of symmetric Kansa collocation is the existence of error bounds. But this method needs the double continuous RBFs and therefore the collocation matrix is built based on the double evaluation of differential operator.

The well-posedness of the asymmetric Kansa method is not guaranteed because the inversion procedure is ill-conditioned for small or big shape parameters. Besides this method can not be applied for strictly conditional positive definite RBFs. Hence we develop a *regularized Kansa method* for overcoming these problems and leading good calibrated results.

## 4 Regularized Kansa collocation method

In this section, we present the main motivation of our methodology for solving SPDEs. Let the multivariate monomial product basis $\mathcal{P}$ for $\mathbb{R}^d$ be denoted by $\prod_{\mathcal{P}}^{m-1}$ and set

$$M = \binom{m+d-1}{d} = \dim(\prod_{\mathcal{P}}^{m-1}).$$

The interest in RBFs comes from the ability of RBF interpolation to approximate a wide range of unknown functions. Actually, the RBF interpolation tries to reconstruct $F$ in the way:

$$F(\boldsymbol{x}) \approx \sum_{j=1}^{N} c_j \Phi(\boldsymbol{x}, \boldsymbol{x}_j) + \sum_{k=1}^{M} d_k P(\boldsymbol{x}).$$

Added polynomial terms to RBF interpolation has two major goals:

1. Passing ill-conditioning problem of inversion at collocation matrix;
2. Global use of conditionally strictly positive definite RBFs.

Due to adding this polynomial term and to ensure the well-posedness, the following condition, known as the orthogonality condition, should be added:

$$\sum_{k=1}^{N} c_k P(\boldsymbol{x}_k) = 0.$$

Hence the matrix form of interpolation can be denoted as:

$$\begin{bmatrix} \mathcal{K} & \mathbb{P} \\ \mathbb{P}^T & \mathcal{O} \end{bmatrix} \begin{bmatrix} \boldsymbol{c} \\ \boldsymbol{d} \end{bmatrix} = \begin{bmatrix} \boldsymbol{F} \\ \boldsymbol{0} \end{bmatrix}, \tag{3}$$

where $\mathcal{K} := \Phi(\boldsymbol{x}_i, \boldsymbol{x}_j)|_{i,j=1}^{N,N}$, the matrix $\mathbb{P}$ is defined by $[P(\boldsymbol{x}_k)]$ for $k = 1, \ldots, N$ , and $\mathcal{O}$ and $\boldsymbol{0}$ are $M \times M$ zero matrix and $M \times 1$ zero vector, respectively.

Now let us apply these setting to a general form of boundary value problem (BVP)

$$\begin{cases} \mathcal{A}u = f, & \text{in } \Omega, \\ \mathcal{B}u = g, & \text{on } \partial\Omega, \end{cases} \tag{4}$$

where the differential and boundary operators $\mathcal{A}$ and $\mathcal{B}$ are continuously defined and $f$, $g$ are source functions for interior and boundary domains, respectively. After applying operators on the interpolation matrix (3), we obtain the collocation system as:

$$\begin{bmatrix} \mathcal{A}\Phi(\boldsymbol{x}_i, \boldsymbol{x}_j)|_{i,j=1}^{N_\rho,N} & \mathcal{A}P(\boldsymbol{x}_j)|_{j=1}^{N_\rho} \\ \mathcal{B}\Phi(\boldsymbol{x}_i, \boldsymbol{x}_j)|_{i=N_\rho+1,j=1}^{N,N} & \mathcal{B}P(\boldsymbol{x}_j)|_{j=N_\rho}^{N} \\ (P(\boldsymbol{x}_j)|_{j=1}^{N})^T & \mathcal{O} \end{bmatrix} \begin{bmatrix} \boldsymbol{c} \\ \boldsymbol{d} \end{bmatrix} = \begin{bmatrix} \boldsymbol{f} \\ \boldsymbol{g} \\ \boldsymbol{0} \end{bmatrix}. \tag{5}$$

## 5 Temporal iterative scheme

In the last section, we present a strong form for solving steady-state BVPs but the real-world problems are dynamic. Hence for the numerical solution to these problems, we need to discretize the problem temporally. Some time discretization schemes are forward Euler, backward Euler, Crank-Nicolson schemes which in this work for having a general form of these schemes, we use the global $\theta$-weighted method.

By taking $n$th instant of evolution as $t_n$ we can discretize (1) as:

$$\frac{U^{n+1}-U^n}{\delta t} = (\theta \mathcal{A}U^{n+1} + (1-\theta)\mathcal{A}U^n) + f^{n+1} + \sigma \frac{W^{n+1}-W^n}{\delta t},$$

where $U^{n+1} := U(t_{n+1}, \boldsymbol{x})$ and so on. As we discussed in the Definition 1, we can set $W^{n+1} - W^n = \xi^{n+1}$, where $\xi^{n+1} \sim Normal(0, \delta t \sigma^2 Q)$ in which $Q$ is the selected covariance function on the interior domain points. Hence, we get:

$$U^{n+1} - \delta t\theta \mathcal{A}U^{n+1} = U^n + \delta t(1-\theta)\mathcal{A}U^n + f^{n+1} + \sigma\xi^{n+1}.$$

After simplification, one can obtain:

$$[\mathcal{I} - \delta t\theta\mathcal{A}]U^{n+1} = [\mathcal{I} + \delta t(1-\theta)\mathcal{A}]U^n + f^{n+1} + \sigma\xi^{n+1},$$

and by taking $U^{n+1} = \boldsymbol{K}\boldsymbol{C}^{n+1}$, we have:

$$[(\mathcal{I} - \delta t\,\theta\mathcal{A})\boldsymbol{K}]\boldsymbol{C}^{n+1} = [(\mathcal{I} + \delta t\,(1-\theta)\mathcal{A})\boldsymbol{K}]\boldsymbol{C}^n + f^{n+1} + \sigma\xi^{n+1}, \tag{6}$$

where $\boldsymbol{K}$ is the interpolation matrix from (3) and its inversion is guaranteed. Besides, since $\mathcal{A}$ is a linear operator, if we consider $\delta t\,\theta$ such that $\|\delta t\,\theta\mathcal{A}\| < 1$ then the inversion of $(\mathcal{I} - \delta t\,\theta\mathcal{A})$ is assured [13]. Therefore by choosing proper temporal sizes, the matrix $[(\mathcal{I} - \delta t\,\theta\mathcal{A})\boldsymbol{K}]$ is invertible. So by setting $\mathcal{M} := [(\mathcal{I} - \delta t\,\theta\mathcal{A})\boldsymbol{K}]^{-1}[(\mathcal{I} + \delta t\,(1-\theta)\mathcal{A})\boldsymbol{K}]$, the tractable iterative scheme can be rewritten as:

$$\boldsymbol{C}^{n+1} = \mathcal{M}\boldsymbol{C}^n + \tilde{f}^{n+1} + \sigma\tilde{\xi}^{n+1}, \tag{7}$$

here $\tilde{f}^{n+1} = [(\mathcal{I} - \delta t\,\theta\mathcal{A})\boldsymbol{K}]^{-1} f^{n+1}$, and $\tilde{\xi}^{n+1} = [(\mathcal{I} - \delta t\,\theta\mathcal{A})\boldsymbol{K}]^{-1}\xi^{n+1}$. We can show the stability of our method by examine $\rho(\mathcal{M}) < 1$ which $\rho$ is the spectral radius.

Finally, the approximation of mean solution can be obtained by:

$$\hat{U}^{n+1} = \boldsymbol{K}^\star \boldsymbol{C}^{n+1},$$

where $\boldsymbol{K}^\star$ is $N^\star \times N$ interpolation matrix with $N^\star$ is the quantity of test points and $\boldsymbol{C}^{n+1}$ is obtained by solving (7).

## 6 Numerical examples

In this section, we study two stochastic evolution equations. The simulations are implemented in MATLAB 2020b program on a Linux Intel Core i5-4200U machine with 4GB RAM. The first considered problem is the one dimensional stochastic heat equation and the second example is the stochastic advection-diffusion problem. A fundamental tool to measure the accuracy and efficiency is the fill distance which is calculated as:

$$h = h_{X,\Omega} := \sup_{x_j \in \Omega} \min_{x_i \in X} \|x_i - x_j\|_2,$$

where $X$ is the trial points set and $\Omega$ is computational space domain.

### 6.1 Gaussian random field

The $\xi^{n+1}$ in scheme (7) is considered as a GRF. In general form if we take a look at all of the time duration, there exists a GRF that is simulated by $\xi^{n+1}$ which in application and implementation is faster and from a probabilistic view, it is theoretically consistent. As we mentioned in Section 2, the inverse multiquadric

$$\Phi(r) = \frac{1}{\sqrt{\epsilon^2 + r^2}},$$

is used for simulation of GRF.

### 6.2 RBF selection

As we mentioned above, RKHS and particularly the native space of any RBF are special. Wendland in [17] described some of these spaces. In this work, our selection is the following *cubic Matèrn* RBF

$$\phi(r) = \exp(-\epsilon r)(15 + 15\epsilon r + 6(\epsilon r)^2 + (\epsilon r)^3), \qquad \epsilon \text{ is shape parameter}$$

which is $\mathcal{C}^6$-continuous. Here, we set the shape parameter as $\epsilon := 0.165\sqrt{N}$, where $N$ is the total number of test points.

The applied error norms to illustrate the efficiency of our method are:

$$L_\infty := \|\mathbb{E}[u(t,x) - \hat{u}(t,x)]\|_\infty,$$
$$RMS := \frac{1}{\sqrt{N}}\|\mathbb{E}[u(t,x) - \hat{u}(t,x)]\|_2.$$

In all the examples, we set $M = 2$, which means we use the monomials $\{1, x\}$.

**Example 1.** Suppose the following one dimensional stochastic heat equation

$$\frac{\partial U}{\partial t} = (\frac{\partial^2 U}{\partial x^2} + f(U)) + \sigma \frac{\partial W}{\partial t}, \qquad \text{in } [0,T] \times [0,1], \tag{8}$$

where $f(U)$ is the non-linear continuous source function. Initial value and boundary conditions can be obtained from analytical mean solution $\mathbb{E}[U(t,x)] = 10\exp(t)x^2(1-x)^2$. We set $\delta t = 0.001$ and absolute error, and standard deviation are calculated at different time, spatial, and statistical realizations.

In Table 1, the numerical errors at $t = 1$ for different values of $h$ and related sample paths $s$ are reported. The evolution of absolute mean error for different time snapshots is illustrated at Figure 1. It is clear that if we set $\sigma = 0$, SPDE changes to PDE which we show this situation in Figure 2. Additionally, as we mentioned above, the numerical stability of our method can be demonstrated by eigenvalues of $\mathcal{M}$ which is depicted in Figure 2.

Theoretically, when the magnitude of realizations (sample paths) grows, the scheme needs to act like the deterministic situation. Indeed, based on mean square continuity definition of stochastic processes, which is defined very well in [15], the regularity of the stochastic process is assured. We show this property of our scheme in Figure 3. In simulations, we set $\delta t = 0.01$ and $s = 1600$. This setting is logical because when realizations go bigger, our scheme becomes deterministic.

Table 1: Numerical study at $t = 1.0$ for Example 1.

| $h$ | $s = sample\,path$ | $L_\infty$ | $RMS$ |
|---|---|---|---|
| $\frac{1}{4}$ | 50 | $2.06137 \times 10^{-1}$ | $1.6828 \times 10^{-1}$ |
| $\frac{1}{8}$ | 200 | $4.62771 \times 10^{-2}$ | $2.22171 \times 10^{-2}$ |
| $\frac{1}{16}$ | 800 | $4.09351 \times 10^{-3}$ | $2.71034 \times 10^{-3}$ |
| $\frac{1}{32}$ | 3200 | $7.90971 \times 10^{-4}$ | $5.65657 \times 10^{-4}$ |

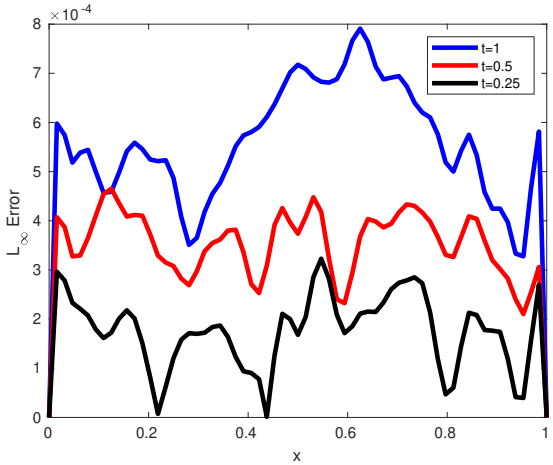


(a) Absolute mean error at $t = 0.25, 0.5, 1.0$ with $h = \frac{1}{32}$ and $s = 3200$ for Example 1.

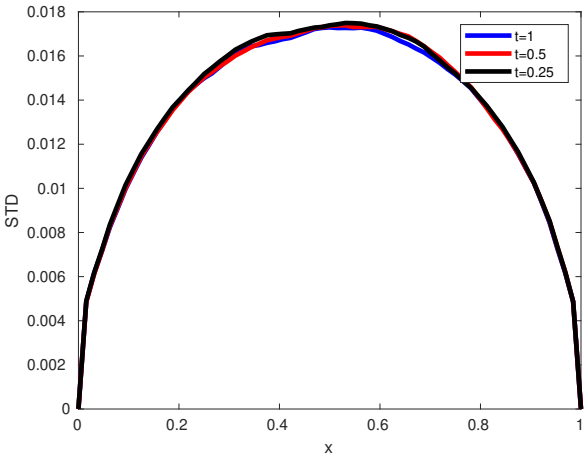


(b) Standard deviation at $t = 0.25, 0.5, 1.0$ with $h = \frac{1}{32}$ and $s = 3200$ for Example 1.

Figure 1: Absolute mean error and Standard deviation for Example 1 at different values.

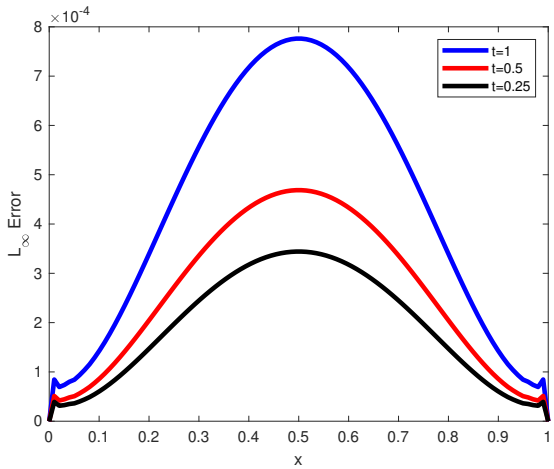


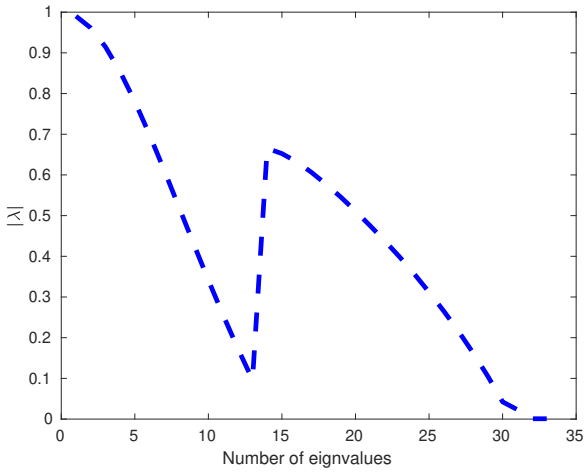


Figure 2: Determinstic solution error and Stability for Example 1.

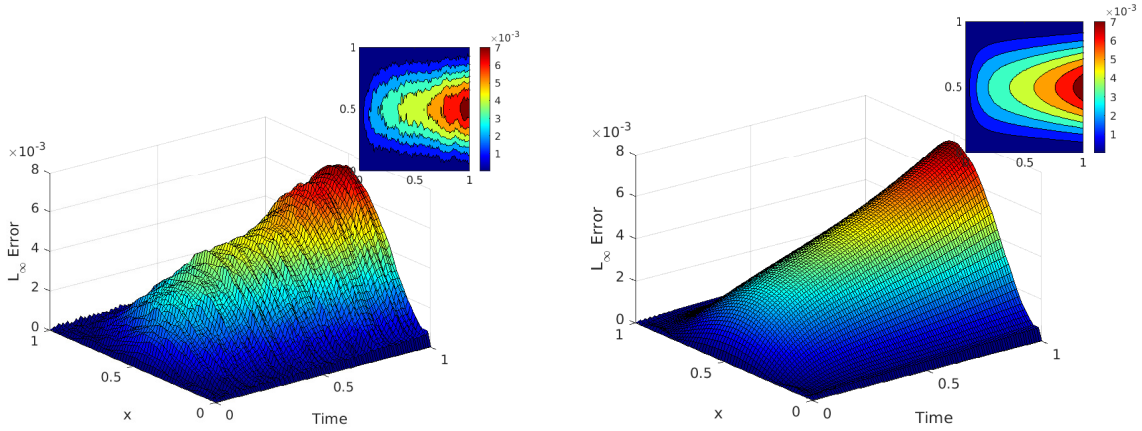


(a) Stochastic (b) Deterministic

Figure 3: Regularity in time of our method through comparison of stochastic solution with deterministic solution for Example 1.

Table 2: Numerical study at $t = 1.0$ for Example 2.

| $h$ | $s$ | $L_\infty$ | $RMS$ |
|---|---|---|---|
| $\frac{1}{4}$ | 50 | $5.8788 \times 10^{-1}$ | $3.38101 \times 10^{-1}$ |
| $\frac{1}{8}$ | 200 | $6.9528 \times 10^{-2}$ | $2.36504 \times 10^{-2}$ |
| $\frac{1}{16}$ | 800 | $9.41844 \times 10^{-3}$ | $4.87357 \times 10^{-3}$ |
| $\frac{1}{32}$ | 3200 | $3.39924 \times 10^{-3}$ | $2.17714 \times 10^{-3}$ |

**Example 2.** Consider the stochastic reaction-diffusion equation as:

$$\frac{\partial U}{\partial t} = (\gamma \frac{\partial^2 U}{\partial x^2} - \nu \frac{\partial U}{\partial x}) + \sigma \partial_t W,$$

where $\gamma$ is the reaction coefficient and $\nu$ is the diffusion coefficient. The expected mean solution or analytical mean solution is given as [16]:

$$\mathbb{E}[U(t,x)] = \frac{1}{\sqrt{4t+1}} \exp\big(-\frac{(x-0.2-\nu t)^2}{\gamma(4t+1)}\big).$$

Through this Example, we set $\delta t = 0.001$. The computed errors for $\gamma = 0.01$ and $\nu = 0.6$ are summarized in Table 2. Also, in Figure 4 absolute mean errors and standard deviations at $t = 0.25, 0.5, 1.0$ are plotted. Additionally, the stability of our method and 15 sample paths of the stochastic solution are shown in Figure 5.

## 7 Conclusion

In the present paper, a collocation method based on the RBF approximation for the numerical solution of the one dimensional stochastic evolution equations has been proposed. The time

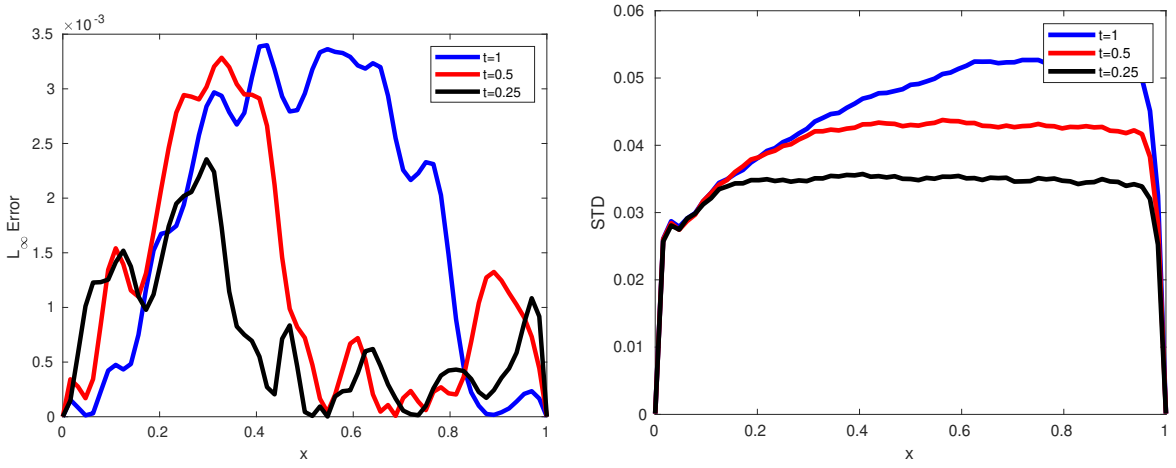


(a) Absolute mean error at $t = 0.25, 0.5, 1.0$ with $h = \frac{1}{32}$ and $s = 3200$ for Example 2.

(b) Standard deviation at $t = 0.25, 0.5, 1.0$ with $h = \frac{1}{32}$ and $s = 3200$ for Example 2.

Figure 4: Absolute mean error and Standard deviation for Example 2 at different values.

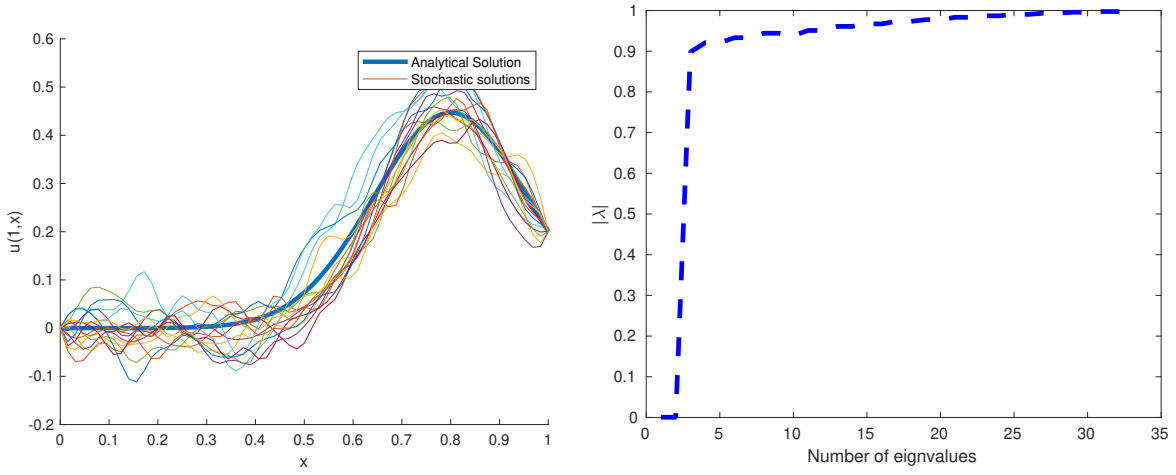


Figure 5: Some of stochastic solutions and Stability for Example 2.

variable was discretized by the global $\theta$-weighted method and meshless collocation was applied on the space variable. The $Q$-Wiener process, which simulates the Gaussian random field (GRF) of the problem, was approximated by Karhunen-Loève expansion. Inverse multiquadric (IMQ) RBF was used as a spatial covariance function for coloring the GRF. Numerical aspects of error analysis were computed by absolute error ($L_\infty$), standard deviation, and root mean square error ($RMS$). The simplicity and strong form of our approach make this method more useful in real world problems. The regularity in time was numerically shown and this regularity makes the presented method statistically consistent.

## Acknowledgements

The authors are very thankful to the reviewers for carefully reading the paper, their comments and suggestions have improved the quality of the paper.

## References

[1] A. Berlinet, C. Thomas-Agnan, *Reproducing Kernel Hilbert Spaces in Probability and Statistics*, Springer, Boston, 2004.

[2] I. Cialenco, G.E. Fasshauer, Q. Ye, *Approximation of stochastic partial differential equations by a kernel-based collocation method*, Int J. Comput. Math. **89** (2012) 2543–2561.

[3] M. Dehghan, M. Shirzadi, *Numerical solution of stochastic elliptic partial differential equations using the meshless method of radial basis functions*, Eng. Anal. Bound. Elem. **50** (2015) 291–303.

[4] M. Dehghan, M. Shirzadi, *Meshless simulation of stochastic advection-diffusion equations based on radial basis functions*, Eng. Anal. Bound. Elem. **53** (2015) 18–26 .

[5] M. Dehghan, M. Shirzadi, *The modified dual reciprocity boundary elements method and its application for solving stochastic partial differential equations*, Eng. Anal. Bound. Elem. **58** (2015) 98–111 .

[6] M. Dehghan, M. Shirzadi, *A Meshless Method Based on the Dual Reciprocity Method for One-Dimensional Stochastic Partial Differential Equations*, Numer. Methods Partial Differ. Equ. **32** (2016) 292–306.

[7] G.E. Fasshauer, Q. Ye, *Kernel-based collocation methods versus Galerkin finite element methods for approximating elliptic stochastic partial differential equations. Meshfree methods for partial differential equations VI*, Lecture notes in computational science and engineering **89** (2013) 155–170.

[8] G.E. Fasshauer, *Solving differential equations with radial basis functions: multilevel methods and smoothing*, Adv. Comput. Math. **11** (1999) 139–159.

[9] T.Y. Hou, W. Luo, B. Rozovski, H.M. Zhou, *Wiener Chaos expansions and numerical solutions of randomly forced equations of fluid mechanics*, J. Comput. Phys. **216** (2006) 687–706.

[10] A. Jentzen, P.E. Kloeden, *The numerical approximation of stochastic partial differential equations*, Milan J. Math. **77** (2009) 205–244.

[11] A. Jentzen, P. Kloeden, *Taylor Approximations for Stochastic Partial Differential Equations*, SIAM, Philadelphia, 2011.

[12] E.J. Kansa, *MultiquadricsA scattered data approximation scheme with applications to computational fluid-dynamicsI surface approximations and partial derivative estimates*, Comput. Math. with Appl. **19** (1990) 127–145.

[13] R. Kress, *Linear Integral Equations*, Springer, NewYork, 2013.

[14] R. Kruse, Y. Wu, *A randomized and fully discrete Galerkin finite element method for semilinear stochastic evolution equations*, Math. Comp. **88** (2019) 2793–2825.

[15] G.J. Lord, E.C. Powell, T. Shardlow, *An Intoduction to Computational Stochastic PDEs*, Cambridge Texts in Applied Mathematics, Cambridge University Press, New York, 2014.

[16] A. Robler, M. Seaid, M. Zahri, *Method of lines for stochastic boundaryvalue problems with additive noise*, Appl. Math. Comput. **199** (2008), 301314.

[17] H. Wendland, *Scattered Data Approximation*, Cambridge University Press, Cambridge monographs on applied and computational mathematics. Cambridge, 2005.